J Ther Eng, Vol. 11, No. 1, pp. 79−93, January, 2025

Journal of Thermal Engineering
Web page info: https://jten.yildiz.edu.tr
DOI: 10.14744/thermal.0000905

Research Article

Performance enhancement of thermal energy storage system using ZrO_2 doped paraffin wax

Shri Krishna MISHRA[1], Mukesh Kumar GUPTA[2], Rahul KUMAR[3,*], Abhishek SHARMA[4]

[1]Department of Mechanical Engineering; Suresh Gyan Vihar University, Rajasthan, 302017, India
[2]Department of Electrical Engineering; Suresh Gyan Vihar University, Rajasthan, 302017, India
[3]School of Mechanical Engineering, Lovely Professional University, Punjab, 144001, India
[4]Department of Mechanical Engineering, Government Engineering College Palamu (Department of Higher and Technical Education, Govt. of Jharkhand), Jharkhand, 822118, India

ARTICLE INFO

Article history
Received: 21 September 2023
Revised: 08 May 2024
Accepted: 13 May 2024

Keywords:
Characterization, Nanomaterial; Paraffin Wax; Synthesis; Thermal Energy Storage

ABSTRACT

The present work focused on the application of zirconium dioxide (ZrO_2), a metal based nano material in a helical tube heat exchanger. A novel nano enhance phase change material (NEPCM) passes through a series of test to explore its energy storage capacity. The aim of the study is to determine the effect of varying amounts of ZrO_2 on the thermal performance of energy storage systems through experiments, and based on the results, to identify the optimal concentration. The scanning electron microscopy (SEM) results indicated that the ZrO_2 physically bonded with paraffin wax without disturbing the chemical stability and structure of the NEPCM samples. It was noticed that ZrO_2 successfully stabilized surface temperature, solidification and melting of paraffin wax. Experiments with ZrO_2 doped with paraffin wax also helped to establish the optimum value of charging and discharging time. The most significant enhancement in charging rate was observed with a mere 0.1–0.3% (vol.) increase, but this enhancement rapidly declined with increases beyond 0.3% in volume concentration. NEPCM with 0.3% concentration in volume was identified as ideal sample. When the mass flow rate increased from 1 to 5 LPM, the exergy efficiency dropped from 21.4% to 15.3%. Compared to other PCM and NEPCM samples, ZrO_2-doped PCM samples exhibited a more favorable thermal response.

Cite this article as: Mishra SK, Gupta MK, Kumar R, Sharma A. Performance enhancement of thermal energy storage system using ZrO_2 doped paraffin wax. J Ther Eng 2025;11(1):79−93.

INTRODUCTION

Energy has been one of the major factors for the development of human civilizations. In the current scenario, economic development of any country is influenced by the energy economics [1]. However, the energy sector confronts significant problems such as increasing usage of fossil fuel, tail pipe emissions and rising price etc. and hence it is necessary to work in the area of finding alternate renewable

***Corresponding author.**
*E-mail address: rahul.aero001@gmail.com

This paper was recommended for publication in revised form by Editor-in-Chief Ahmet Selim Dalkılıç

sources [2, 3]. Over the last few decades, researchers from all over world have been looking for innovative technologies that will help to reduce the use of fossil fuels and, as a result, reduce negative impact on climate and the environment due to burning of fossil fuels. Energy storage is one of suitable strategies for storing the renewable energy which would help to replace the usage of fossil fuel [4–6]. One of the utmost popular energy storage technologies is thermal energy storage (TES). Latent heat thermal storage (LHTS) and sensible heat storage are the two categories under TES [7]. The amount of energy stored per unit mass when a material goes through a phase transition is equal to the integral of the substance's specific heat times the temperature gradient. The volume of medium needed to store the same amount of energy via sensible heat transfer is more than what is needed via latent heat transfer [8, 9].

Thermoelectric ZrO_2 nanoparticles have several significant uses in this area. During phase transitions, phase change materials can store and release thermal energy; ZrO_2 nanoparticles can be integrated into these materials. As a whole, the PCM is better able to release and store thermal energy because the nanoparticles increase their thermal conductivity [10]. The thermal conductivity of heat transfer fluids can be improved by adding ZrO_2 nanoparticles to them. Applications that rely on efficient heat transfer for energy storage, like concentrated solar power and solar thermal systems, find this feature particularly valuable. Zirconium dioxide nanoparticles are a potential component of high-tech materials for thermal energy storage. During times of abundant energy, these systems collect and store excess heat, which they then release when needed [11]. Such storage systems benefit from ZrO_2 characteristics, which enhance their efficiency and thermal performance. In thermochemical energy storage devices, ZrO_2 nanoparticles can be utilized to store and release heat energy through chemical reactions. With this method, heat can be efficiently stored for use at a later time [12].

These two solutions are not technically feasible due to the low latent heat of solid-solid conversion and the high volume needed for liquid-gas conversion. Additionally, we will exclusively refer to energy storage through the solid-liquid transformation since it has a larger density and functions at a constant temperature of PCM. PCM mostly focuses on latent heat storage, whereas sensible storage of heat depends on changes in material temperatures [13, 14]. Large amounts of energy can be stored and released using thermal energy storage via PCM. Energy storage and release are influenced by the materials' phase changes. Practical tests have demonstrated that as compared to sensible heat storage, PCM can achieve a significant reduction in storage space [11, 12]. Aadmi et al. [13] composites of paraffin wax and epoxy resin were investigated using a hot plate device in both experimental and numerical (using Comsol Multiphysics) settings. Melting of PCM was found to be affected by the shape of the container, and it was found that increasing the PCM content in the mixture increased the LHTES's efficiency. Randeep et al. [14] performed experiments to improve the thermal conductivity of PCM using a storage system with aluminium and graphite fins. Also, carbon power was added with PCM. It was found that for pure PCM samples, the melting started at 37°C and continued to above 40°C. Purohit and Sistla [15], in an experimental and computational analysis of a PU-PCM composite's thermal characteristics, salt hydrate was found to dominate the nucleation and crystallization processes. Herbinger et al.[16], In numerical analysis of an air-PCM heat exchanger using dodecanoic acid, it was found that smaller heat exchanger channels and hotter air resulted in a higher heat transfer rate. Sun et al. [17] examined how PCM incorporated LBW affected energy use in humid settings. When the humidity rose from 40% to 90%, energy savings were seen to drop from 1.64 percent to 1.32 percent, however, the difference was not statistically significant during the winter. Fateh et al. [18] investigating effects of the solar radiation (which was viewed as the boundary's time-varying heat source) led researchers to the conclusion that the right PCM may reduce the heating load by 75%. Kishore et al. [19] examined a significant impact on how well PCM performs, as well as PCM location, phase-conversion temperature, latent heat, and thickness. Zwanzig et al. [20] energy-saving potential analysis revealed that PCM performance is highly dependent on weather conditions, emphasizing the need to choose alternative PCMs in various climate zones. An experimental and numerical analysis found no cracking in the PCM's spherical shell, which contained various characteristics generated via KNO_3-$NaNO_3$ [21]. Wang et al. [22] examined the thermal performance of PCM wall panels in Shanghai's lightweight structures with regard to phase-conversion temperature, and thickness with the use of Energy Plus's single-zone model. It was discovered that optimal phase-transition temperature differed depending on the room's location and changed throughout the year owing to variations in solar radiation levels. Yahya Ali Rothan [23] investigated how fins and nano-powders can be used to improve the freezing of PCM. To enhance the performance of PCM, a nano powder of CuO was added to the mixture. The time required to freeze water was found to decrease by 5.49% for every unit increase in form factor. It was also shown that an 11% reduction in processing time can be attained by increasing the CuO content. In another study by Arena et al. [24], Heat transfer by convection, laminar flow, and turbulent flow were all studied in mushy zone of a finned double-pipe LHTES using paraffin RT35. A decrease in natural convection was seen during the charging and discharging heat cycles for larger values of the mushy zone constant, which represents the mushy region. Youssef et al. [25] employed a PCM heat exchanger with spiral wiring tubes in the experiment and also produced a CFD model for a TES system with composite epoxy resin spherical form paraffin wax RT27. Validation of the Experiment and CFD simulation outcomes followed. With this layout, it was discovered that PCM's thermal

conductivity could be improved and that PCM could move freely, resulting in better heat transmission. Zhou et al. [26] Using an enthalpy method model, researchers looked at how varying PCM parameters affected the attenuation coefficient and delay time in shape-stabilized PCM. They found that the phase-transition temperature was a major influence on the evaluation index, and that, for a given external heat disturbance, there were relatively optimum values for the latent heat of PCM.

Woloszyn et al. [27] improved thermal energy storage capacity of a PCM shell and tube system by installing a double-tube heat exchanger. Eight distinct design solutions were compared for melting time and exergy efficiency. Comparing PCM melting times with those of vertical, horizontal, and helical coiled systems revealed a considerable improvement. Arena et al. [28], Both charging and discharging partial loads of LHTES systems have been analysed. When the melting fraction was between 0.75 and 0.90, the thermal cycle time was cut by up to 50%, and the amount of energy stored was cut by up to 30%. Veraz et al. [29] established a system for storing thermal energy by placing two rectangular slabs of uniform length and width into a tank of varying thickness. According to the data, employing thinner slabs has enhanced power, which has reduced charging and discharging times by 14 and 30 percent, respectively. Jagganath and Dinesh [30] examined the various phase change materials utilised in thermal energy storage devices to improve thermal performance. System efficiency, heat absorbed and rejected while charging, and temperature swings during discharging were all compared. It was discovered that, under the same conditions as paraffin wax, fatty acids have superior performance characteristics. Williams and Peterson [31] studied PCMs with a focus on their phase transition temperature, rheological effects, and chemical stability. Charging and discharging times for organic PCMs were found to be shortest when they contained either metallic nanoparticles or carbon-based nanoparticles. The goal of researchers is to find solutions to problems and new ways to make things better. Possible gaps in the literature are as follows: Further research into the optimal combination of different nanomaterials with paraffin wax to enhance its thermal characteristics may be necessary. This may necessitate testing varying quantities, sizes, and kinds of nanomaterials. Although it is well-established that nanomaterials improve thermal conductivity, there may be knowledge gaps about the exact processes and interactions that cause this improvement. It is critical to conduct additional in-depth research on the chemical and physical interactions between paraffin wax and nanoparticles. Additional research could focus on determining the effects of various nanomaterials on the nucleation and crystal formation induced by phase transitions in paraffin wax. A careful selection and testing of the nanomaterial is still necessary, even though the literature review suggests nanoparticles as promising catalysts or thermal conductivity enhancers[32–35].

The previous studies suggested that the optimal combination of different nanomaterials with paraffin wax to enhance its thermal characteristics is essential. This may necessitate testing varying quantities, sizes, and variety of nanomaterials. Although it is well-established that nanomaterials improve thermal conductivity, there may be knowledge gaps about the exact processes and interactions that cause this improvement. Further, the effects of various nanomaterials on the nucleation and crystal formation induced by phase transitions in paraffin wax can be carried out. A careful selection and testing of the nanomaterial is still necessary, despite the fact that literature review suggests nanoparticles as promising catalysts or thermal conductivity enhancers [39–42]. The optimal nano inclusion concentration has received little attention from researchers

It can be concluded from the literature that there is no apparent pattern for thermal performance of the NEPCM, despite the fact that oxides, and carbon-based nano additives exhibited good performance. Even more difficult is the identification of a class of nano additives and a potential nano additive that can deliver stable thermal performance. Based on the above literature review, the aim of the study is to utilize varying amount of ZrO_2 nano material to enhance the performance of PCM. The nano enhanced phase change material (NEPCM) was used in a helical tube heat exchanger to conduct both experimental and theoretical research on metal oxide-based NEPCM samples. The experimental study seeks to calculate the ideal volume concentration for the desired performance, while the empirical investigation measures the impact of temperature gradient and viscosity on the solidification and melting times, total enthalpy and heat flux of NEPCM samples.

EXPERIMENTATION PROCEDURE

Selection of Material

Paraffin is used as the base in all of the experiments. Nanoparticles of three metal oxide concentrations of ZrO_2 are infused into the paraffin to improve its performance. Table 1 lists the requirements, such as particle size and purity, that the material provider requires. Table 2 lists the individual characteristics of nano inclusions and PCM basis. When we receive the Material from the manufacturer, it is in its unprocessed form. Table 3 displays the total weights of all three ZrO_2-PCM samples generated at the different volume concentration of 0.1 to 0.3%. Thermodynamic stability, excellent thermal conductivity, and environmental toughness are the main reasons why ZrO_2 nanoparticles are used for thermal storage. Compare nanomaterials to zirconium dioxide by their properties, applications, and benefits. Applications requiring high-temperature stability can use zirconium dioxide's high melting point. Consider application criteria including thermal stability, biocompatibility, and electrical qualities when comparing ZrO_2 to other nanomaterials.

Table 1. Material supplier details

Zirconium Oxide (ZrO_2)	99.9%	Platonic Nanotech Pvt. Ltd
Paraffin	99.9%	Platonic Nanotech Pvt. Ltd

NEPCM Samples Preparation

NEPCM samples are first prepared by determining how much nanomaterial will be added to the paraffin solvent. The authors here create numerous samples of ZrO_2 doped PCM with volume concentrations increasing of 0.1%, 0.2%, and 0.3% to examine the effects of nano inclusions in base paraffin. After 1.5 hours of magnetic stirrer and 2.5 hours of ultrasonication, the samples are treated to base paraffin to confirm complete diffusion of the nanomaterial. The PCM samples are maintained throughout the entire procedure in a liquid condition by maintaining a constant temperature of 65°C during both phases. Zirconium oxide nanoparticles and paraffin wax are combined to create a nano-enhanced phase change material (NEPCM), which improves the thermal characteristics of wax. The general procedures for making a NEPCM sample using paraffin wax and zirconium oxide nanoparticles are listed below. Select zirconium oxide nanoparticles with good thermal conductivity and compatibility with paraffin wax. The performance of the NEPCM can be affected by the nanoparticles' size and surface properties. Zirconium oxide nanoparticles should be dispersed in an appropriate solvent. In order to keep nanoparticles from clumping together, this dispersion stage is crucial. To improve stability, surfactants or dispersion agents might be used. Add the scattered zirconium oxide nanoparticles to the melted paraffin wax after it has melted. To promise that nanoparticles are consistently dispersed throughout in paraffin wax, thoroughly stir the mixture. Once everything is ready, the heat exchanger is filled with the samples, as depicted in Figure 1 (a) and (b).

Table 2. Materials thermo-physical parameters

Parameters	PCM	ZrO_2
Size(mm)		30-50
Density (Kg/m^3)	750 (liquids)	1300
	880 (solids)	
Thermal conductivity (W/m. K)	0.2 (liquids)	13.0
	0.2 (solids)	
Temperature(°C)	43.0	1000
Latent heat (KJ / Kg)	260.0	-
Specific heat (KJ/Kg. K)	2.31	-

Table 3. Paraffin and nanomaterial samples weight

Samples of NEPCM	Nanomaterial Quantity (grams)	Paraffin Quantity (grams)
99% Paraffin+.1% ZrO_2	24.7	7478.2
98% Paraffin+.2% ZrO_2	68.4	7434.5
97% Paraffin+.3% ZrO_2	114.8	7388.1

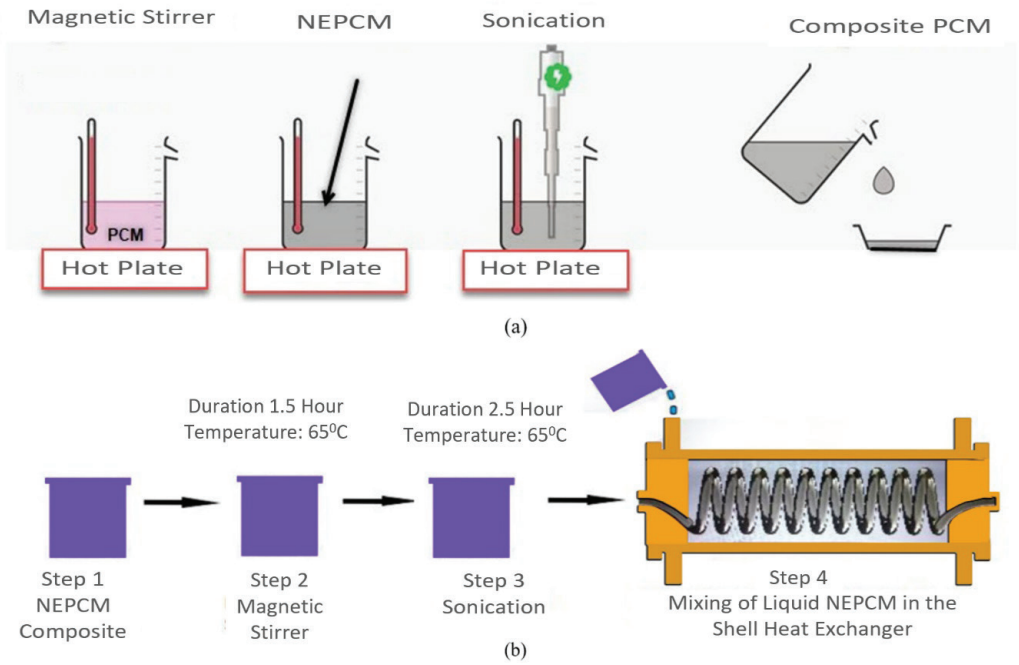

Figure 1. Diagram for preparing samples of NEPCM.

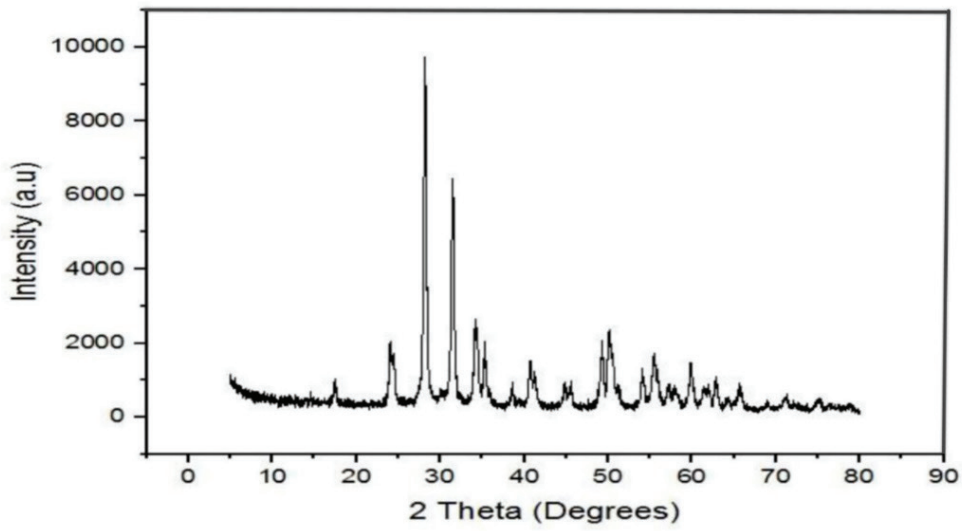

(a)

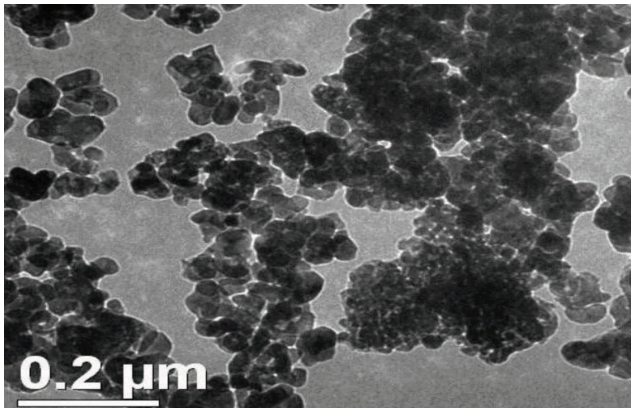

(b)

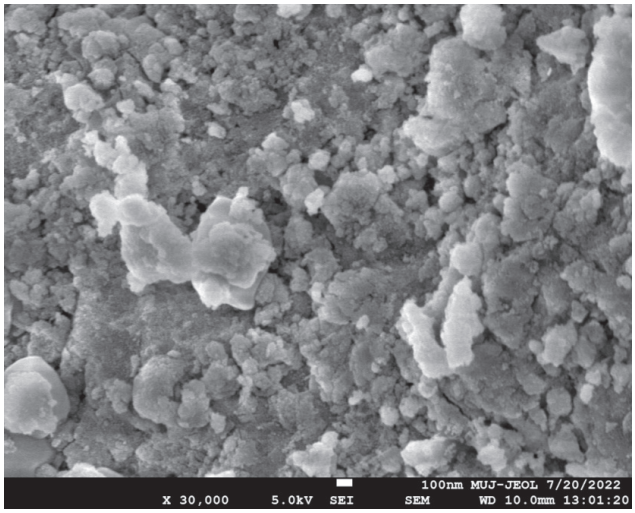

(c)

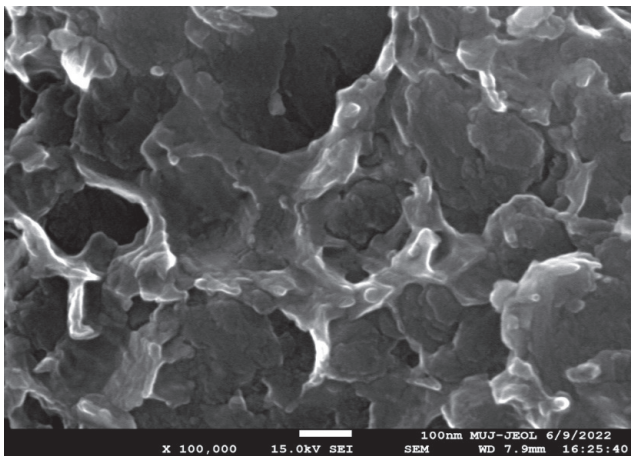

(d)

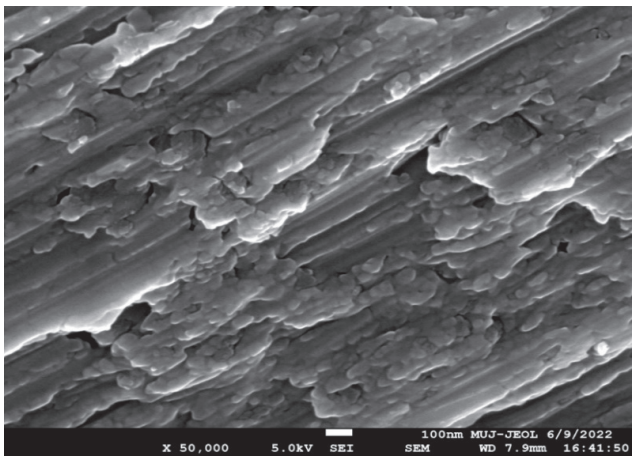

(e)

Figure 2. (a) XRD of Zirconium Oxide Nanoparticles, (b) TEM analysis of the ZrO_2 nanoparticle, (c) 0.1 % Zirconium oxide with Paraffin Wax, (d) 0.2 % Zirconium oxide with Paraffin Wax, (e) 0.3 % Zirconium oxide with Paraffin Wax.

The effect of adding nanoparticles of metal oxide varying in size from 5 nm to 100 nm is the focus of the current research. Previous research has shown that reducing particle size in NEPCM samples enhances the possibility of collision between nanoparticles and base paraffin, which increases the surface area and, in turn, improves the performance of the NEPCM samples.

ZrO_2-PCM Characterization

The XRD analysis of the zirconium oxide material is shown in Figure 2(a) based on common crystal structures, it can explain what an X-ray diffraction (XRD) pattern for zirconium oxide nanoparticles would resemble. There are various crystal phases of zirconium oxide (ZrO_2), and the XRD pattern is dependent on the particular phase that is present. With peak shifts, the diffraction peaks resemble those of monoclinic zirconia. distinct peaks at 30.2°, 35.1°, 50.0°, and 60.0° around 2θ values. Furthermore, zirconium oxide nanoparticles may display a mixture of phases, and peaks corresponding to different crystal structures may be seen in the XRD pattern. TEM analysis shows in the Figure 2(b) of the zirconium nanoparticle. One effective tool for investigating nanoscale material structure and morphology is transmission electron microscopy, or TEM. Nanoparticle size, shape, and distribution can be studied in great detail by transmission electron microscopy (TEM) images. Dark spots in the transmission electron micrograph will be the zirconium oxide nanoparticles. It is also possible to tell if the nanoparticles are round, rod-shaped, or otherwise irregular in shape. The crystalline structure of the material can be indicated by the presence of well-defined lattice fringes within individual nanoparticles. If the nanoparticles clump easily or are evenly distributed. The different percentage of the ZrO2 with paraffin wax samples the SEM image shows in the Figure 2(c), 2(d) and 2(e) respectively. Images obtained by scanning electron microscopy illustrate the structure of the zirconium oxide nanoparticles embedded in the paraffin wax. Agglomerates, clusters, or solitary spheres might be how nanoparticles appear. It demonstrates how composite materials are evenly distributed. You can see the paraffin wax matrix's surface structure. It checks for changes in smoothness, texture, or other properties brought about by nanoparticle addition. Using scanning electron microscopy (SEM), the presence or absence of agglomeration of zirconium oxide nanoparticles can be seen, providing insight into their dispersion and clustering behavior. Sample preparation methods, such as the use of an appropriate coating to increase conductivity and decrease charging effects, are critical to obtaining high-quality SEM images.

Experimental Setup

An investigational setup including a PCM tank and heat source tank used heat transfer fluid storage pipeline arrangement, control unit, and data recording unit is designed to study the temperature and performance of NEPCM samples in heat exchanger. To keep the charging process's temperature constant, water heaters employ an electric heater that is digitally regulated. The heat exchanger is built of copper tubes and a stainless-steel casing. The heat exchanger's dimensions are 140 mm in cell dia., 2 mm in thickness, and 450 mm in length. The heat exchanger's helical copper tubes have a thickness of 8.6 mm with 17-18 turns. The goal is to document the sample temperature difference between the HTF and the NEPCM. The figure of the experimental set-up as shown in the Figure 3(a), and the Figure 3(b) shows internal structure of the thermal store cylinder. RTD-based sensors are placed to record the temperature changes in HTF and the inlet and outlet temperatures of the NEPCM samples. At both ends of the spiral coil, another set of sensors has been attached. Water flow from HTF tank to heat exchanger is controlled manually, and the hot and cold circuits of heat exchanger both measure mass flow rate. The systems feature switches for controlling the various heating and pumping mechanisms as well as a control unit with a temperature display, a flow rate display, and these displays.

Experimental Procedure

The municipal supply water is flowing through heat exchanger before the charging cycle begins to establish a base temperature from which all subsequent melting cycles can be measured. The supply water is then pumped into the HTF tank, and electric heaters bring the water to the ideal temperature. The tubes of heat exchanger are recirculated with heated fluid by centrifugal pump. With the help of the valves, we may control the fluid's mass flow rate.

In present study, the charging cycle was tested at different intake temperatures (49°C) and three different mass flow rates (1.0, 2.0,3.0, 4.0 and 5.0 l/min) for each NEPCM sample. NEPCM samples absorb the fraction of latent heat energy of fluid and start melting, confirming absorption of the thermal energy by PCM, when a hot fluid transfers heat energy to the NEPCM sample, causing the NEPCM temperature to rise and the output temperature of the HTF to fall. Even more HTF is sent back, and this keeps happening until all the temperature sensors show temperatures higher than PCM's melting point. The charging process is terminated once the set temperature is reached.

By pumping 50°C HTF fluid through the heat exchanger's tubing, the benchmark temperature is established at the start of the discharging cycle. The heat exchanger tubes are then opened up to allow for the passage of cold water at 15°C. The NEPCM emits heat energy, which is absorbed by the cold water. After it begins to harden, its temperature drops while the HTF temperature rises. While the liters of water discharged per minute may vary between cycles, the pace at which they are discharged remains constant at 1, 2, and 3 liters.

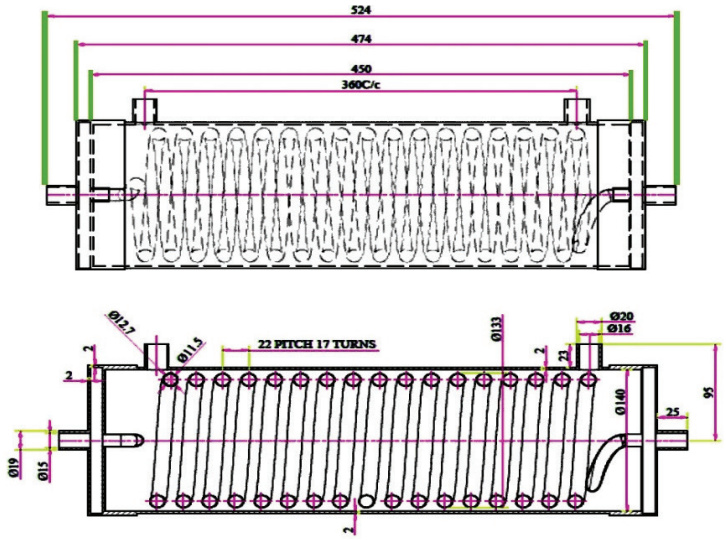

(a)

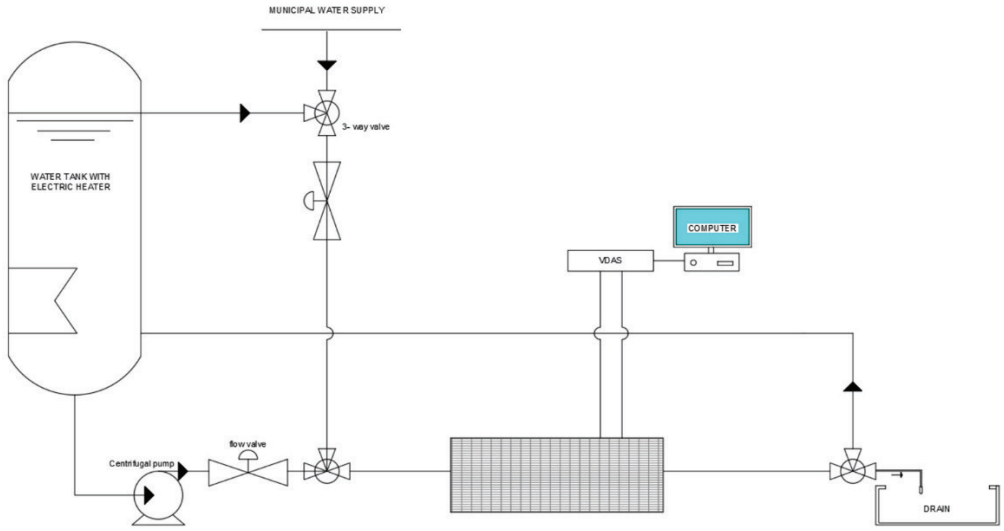

(b)

Figure 3. (a) Schematic Diagram of the energy storage system, (b) Design Model of TES cylinder (all dimensions in mm).

Data Reduction

Mathematical formulation of energy and exergy

A mathematical explanation of the melting and solidifying processes is provided here, [43–45]:

$$E_{inlet} = \dot{m}\, C_F \int_0^t [T_{inlet} - T_{outlet}]dt \quad (1)$$

$$E_{outlet} = \dot{m}\, C_F \int_0^t [T_{outlet} - T_{inlet}]dt \quad (2)$$

The heat absorbed by water is represented by Eout, and the heat absorbed by the PCM is represented by Ein. The fluid's mass flow rate is m, and its specific heat is CHTF.

The storage tank's thermal efficiency can be calculated as

$$\eta = \frac{E_{outlet}}{E_{inlet}} \quad (3)$$

You may calculate energy using the following formulas [46,47].

$$X_{inlet} = \dot{m}C_F \int_0^t [\,(T_{inlet} - T_{outlet}) - T_0\, ln\,(\frac{T_{inlet}}{T_{outlet}})] \quad (4)$$

$$X_{outlet} = \dot{m}C_F \int_0^t [\,(T_{outlet} - T_{inlet}) - T_0\, ln\,(\frac{T_{outlet}}{T_{inlet}})] \quad (5)$$

$$X_{stored\ energy} = \dot{m}C_{HTF} \int_0^t [\,(T_{inlet} - T_{outlet})\,(1 - \frac{T_0}{T_{melting}})]dt \quad (6)$$

Tin and Tout, Tmelt and To are the input and output temperatures, as well as the melting and room temperatures,

respectively. A TES unit's charging, discharging, and overall efficiencies can be found using the following formulas [48]:

$$\varepsilon_{charging} = \frac{X_{stored}}{X_{inlet}} \quad (7)$$

$$\varepsilon_{discharging} = \frac{X_{outlet}}{X_{stored}} \quad (8)$$

Uncertainty analysis

δR, the total uncertainty of the experimental data is influenced by multiple factors. (X_1, X_2,..., X_n); The measurement error of an individual, represented by X_n, is computed as follows [49]:

$$\delta R = \sqrt{\sum_{n=1}^{N} \left(\frac{\delta R}{\delta X_n} \delta X_n\right)^2} \quad (9)$$

The capacity, charging, and discharging uncertainties related to volumetric thermal storage were examined in this work. The volume measurement was accurate to within 1%. As a result, the maximum uncertainties for Einlet and Eoutlet were 3.25% and 3.48%, respectively, and the maximum uncertainties for charging and discharging were 20% and 22%.

RESULTS AND DISCUSSION

PCM Charging Process

Charged PCM will be used to store latent heat later on. To do this, water is heated to the proper temperature using electric heaters before being pumped through a bed of PCM using a centrifugal pump. The PCM bed is heated by the hot

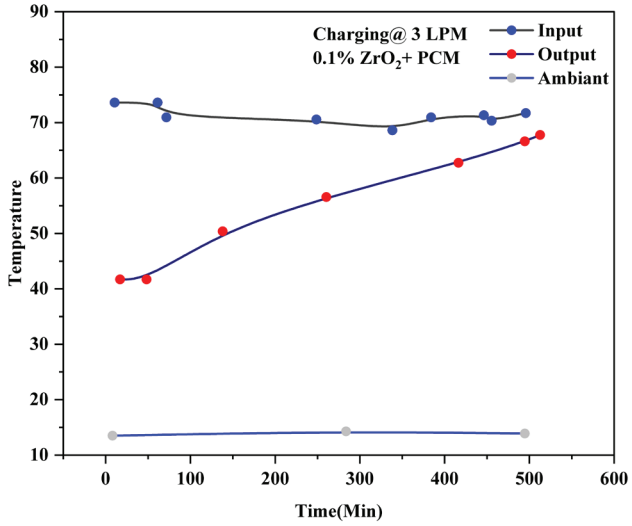

(a)

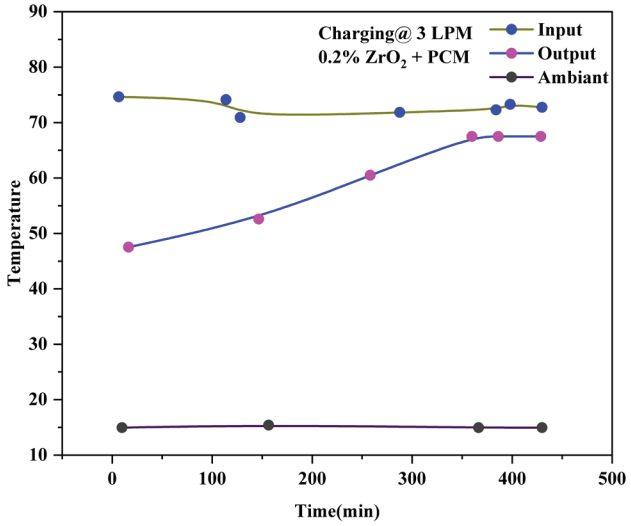

(b)

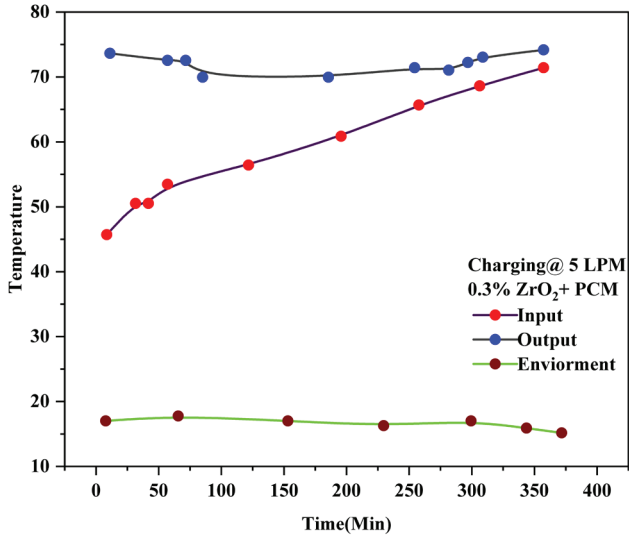

(c)

Figure 4. (a) During charging 0.1 percentage of ZrO_2 PCM temperature, (b) During charging 0.2 percentage of ZrO_2 PCM temperature, (c) During charging 0.3 percentage of ZrO_2 PCM temperature.

HTF. PCMs start melting when they absorb the latent fraction of heat and experience a phase conversion from solid to liquid. Multiple flow rates are used to charge the PCM bed, and this process is repeated until bed temperature reaches 75°C. The process was carried out at a temperature of 32°C to 34°C. The PCM bed was instrumented with a thermocouple, which was then submerged into the PCM, and the resulting data was recorded in the PCM's enclosing glass. The charge of the encapsulated PCM accelerates with increasing HTF flow rate, and charging time decreases, as illustrated in Figure 4(a), 4(b) and 4(c), respectively.

Discharging Process

This discharging operation is performed to remove heat from the PCM bed. It all started with pumping cold water through the PCM bed from the top down. Here, the encased PCM begins hardening as the residual heat it contains is released. In addition, a higher HTF flow rate speeds up the process. There is an initial assumption that both the PCM input and the surrounding air temperature are 34 °C. Discharging continues to raise HTF temperatures, though. This procedure is repeated until the HTF reaches a temperature of 34°C. The discharging of the different nano samples is shown in Figure 5(a), 5(b), and 5(c) respectively.

Mass Flow Rate Impact on Multiple PCM

The encapsulated PCM with progressively higher melting temperatures are employed as the thermal energy storage system in this investigation. Keeping HTF from

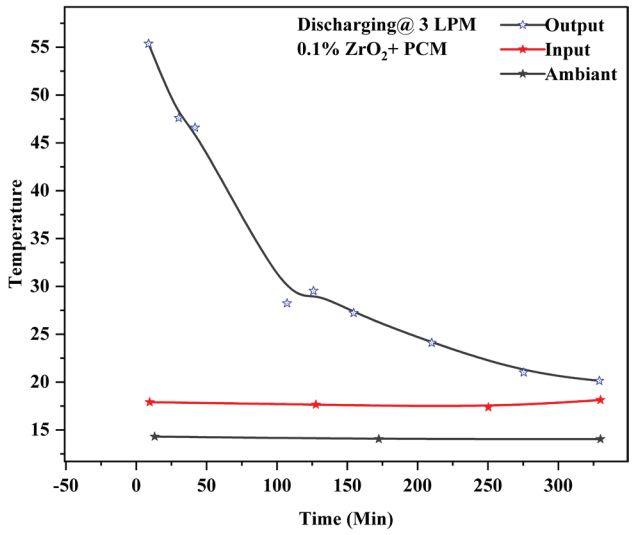

(a)

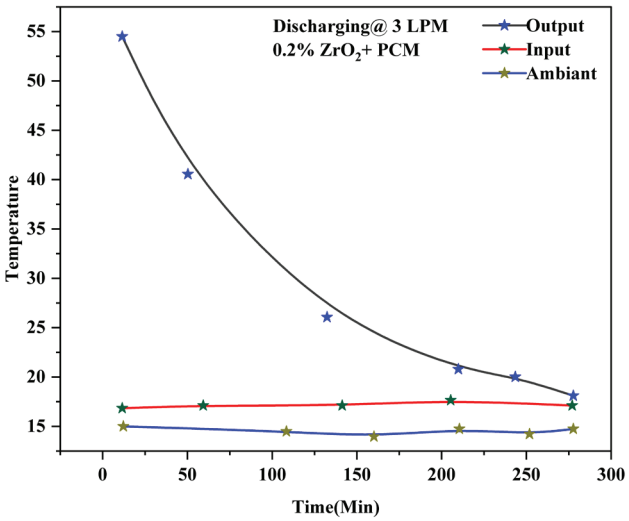

(b)

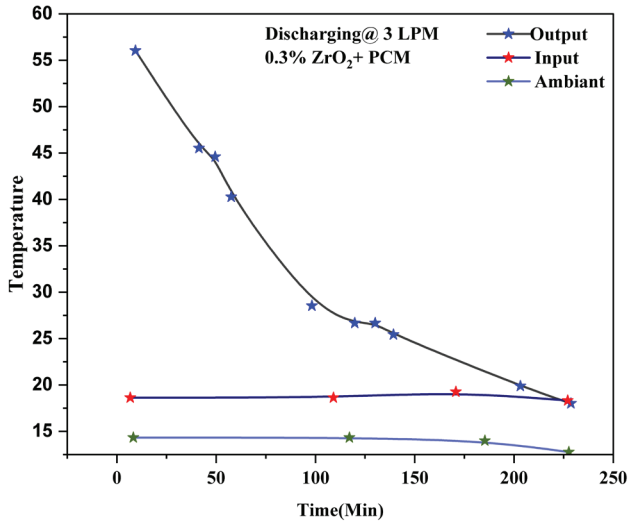

(c)

Figure 5. (a) During discharging 0.1 percentage of ZrO_2 PCM temperature, (b) During discharging 0.2 percentage of ZrO_2 PCM temperature, (c) During discharging 0.3 percentage of ZrO_2 PCM temperature.

overheating necessitates using three distinct layers. The temperature distribution in the PCM capsule-filled packed bed is depicted graphically in the PCM diagram. Increase the flow rate to hasten the charging of your thermal energy system. It was observed that the difference in temperature between HTF and PCM is crucial to the success of heat removal and heat transfer operations. In event of multiple PCM, the HTF begins melting, when it reaches PCM. As can be seen in Figures 6(a) and 6(b), as well as Figure 6(c), different percentage PCM layouts simplify the charging and discharging procedure. Figure 6(d) depicts the relative differences in melting time between different HTF temperatures.

Energy and Exergy Analysis

The amount of energy the HTF puts into and takes out of PCM during the charging and discharging cycle is calculated using Equations (1) and (2). The results of applying Eq. (3) on values of the important constraints and the TES system's complete effectiveness. As the mass flow rate rises, charging efficiency rises with it. However, as can be seen in Figure 7(a), the overall efficiency and rate of discharge are both reduced. The input-output and stored exergy during discharging and charging are given by Equations (4), (5), and (6). The efficiency with which exergy is provided during charging and discharging is shown by Equations (7) and (8). As demonstrated in Figure 7(b), the exergy efficiency of the TES system falls as the mass flow rate rises.

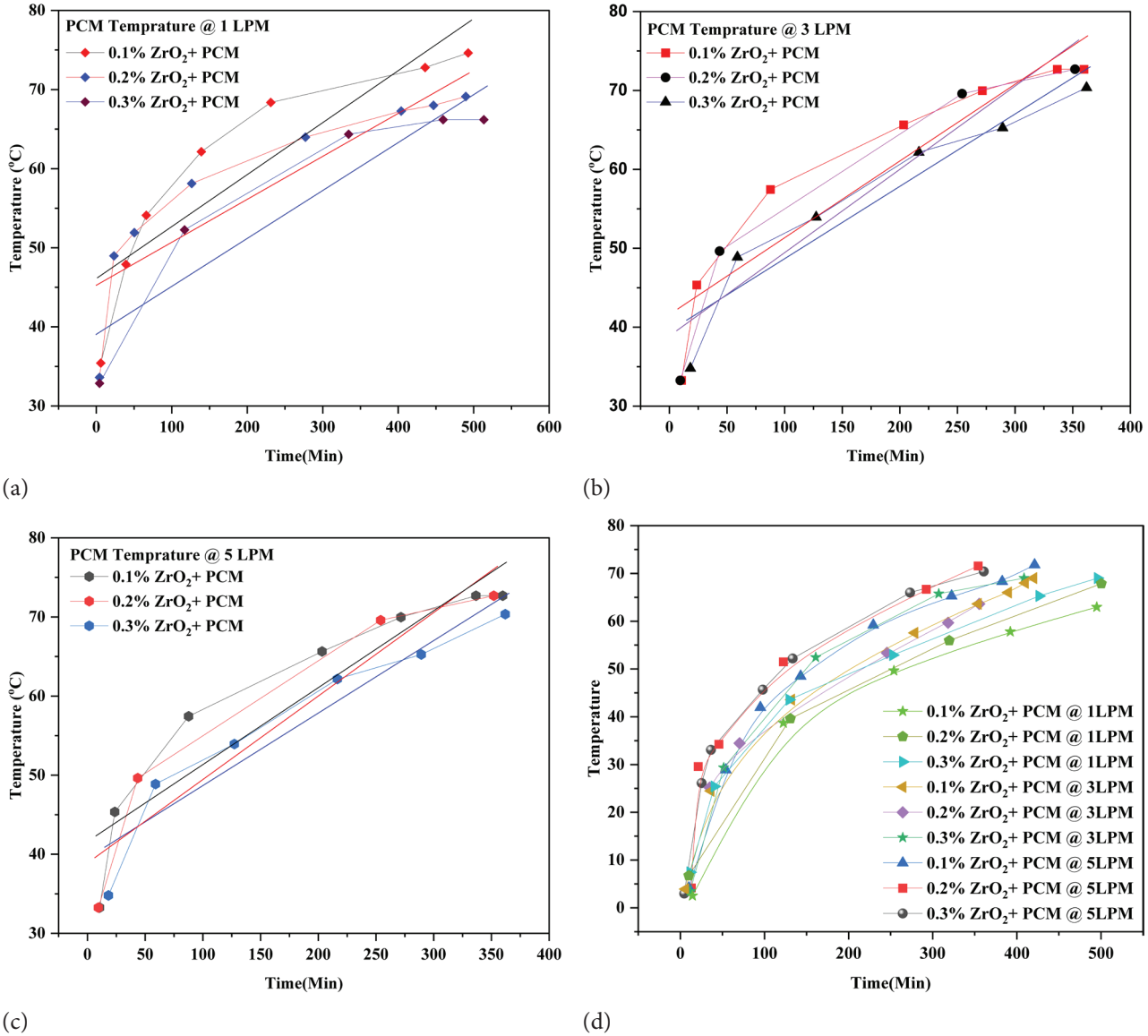

Figure 6. (a) Different percentage of ZrO_2 PCM temperature during charging at 1 LPM, (b) Different percentage of ZrO_2 PCM temperature during charging at 3 LPM, (c) Different percentage of ZrO_2 PCM temperature during charging at 5 LPM, (d) Comparison of different percentage of ZrO_2 PCMs temperature varies with various flow rate.

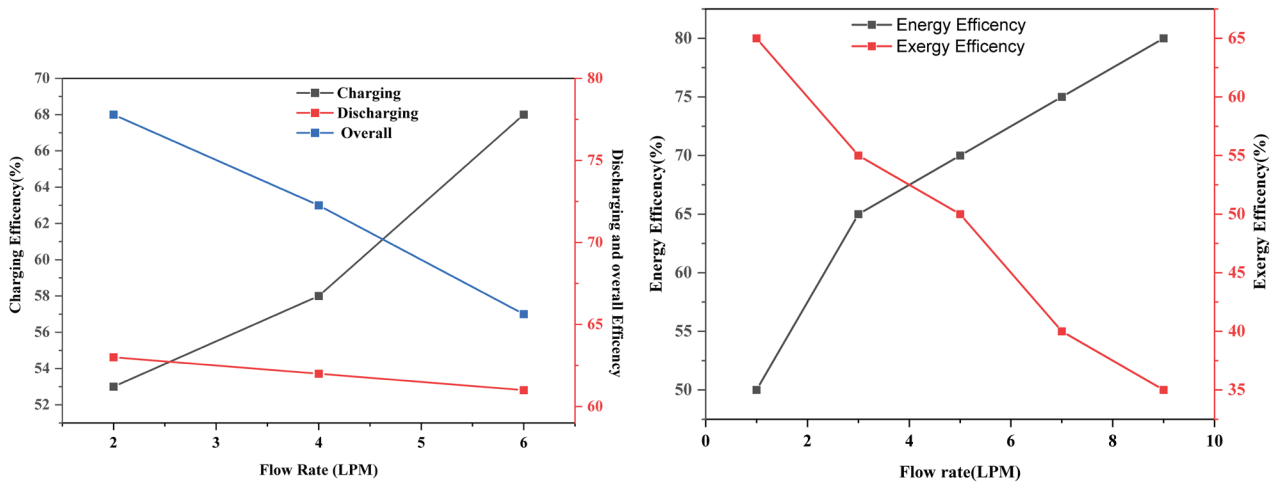

(a) (b)

Figure 7. (a) Variation of flow rate vs Overall efficiency and charging-discharging, (b) Exergy efficiency and HTF flow rate variation.

Effect of Liquid Fraction Variation in NEPCM (ZrO_2 and PCM)

Figure 8 displays the results of a simulation of the thermal storage cylinder with a single NEPCM for the liquid portion. Melting occurs faster than it does on the outlet side, as predicted. This is because natural convection lowers the temperature of the moving fluid while keeping the energy storage area constant. The quantity of latent heat stored or released by the NEPCM depends on the liquid fraction directly. The proportion of liquid in the PCM changes when it changes from a solid to a liquid state (melting) or from a liquid to a solid state (solidification). NEPCM remains able to store and release more energy per unit mass than traditional materials maintaining stable temperatures because of the increased latent heat being stored or released when a higher liquid percentage is present. Therefore, the melting process is enhanced by the addition of the input side tube. Figure 9 depicts the effects of liquid fraction application at the intake and outflow on PCM solidification. The findings suggest that the nanoparticles facilitate solidification and that their length decreases the phase transition time. Heat conduction and enhanced heat transfer surface area are responsible for the enhancement. The liquid fraction variation can influence the thermal response time of the

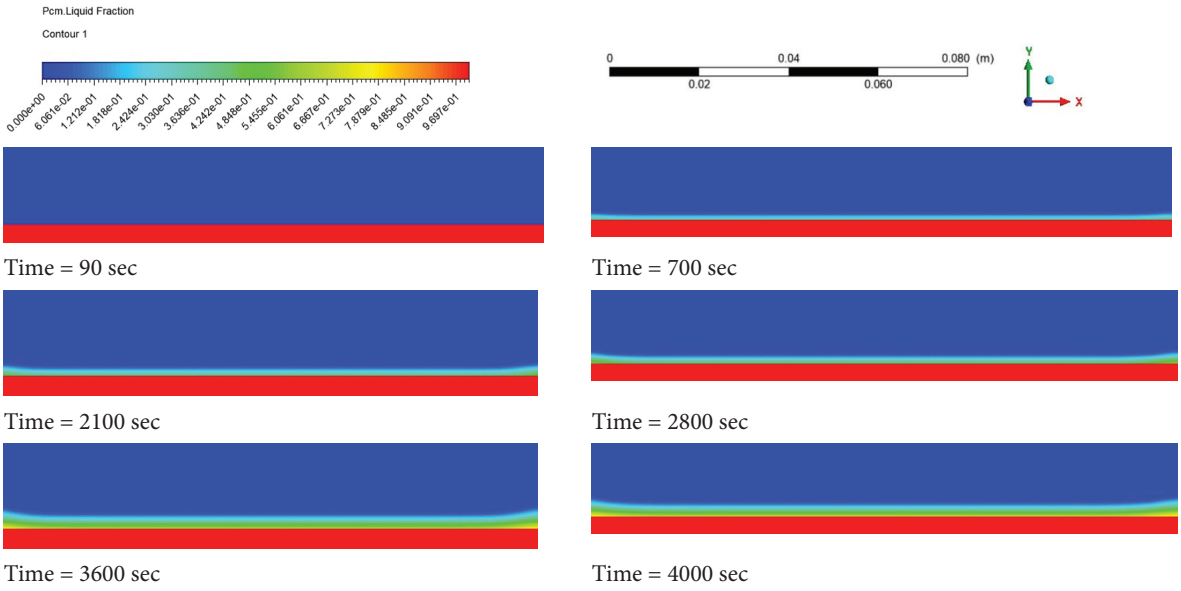

Figure 8. Liquid fraction simulation of NEPCM storage material.

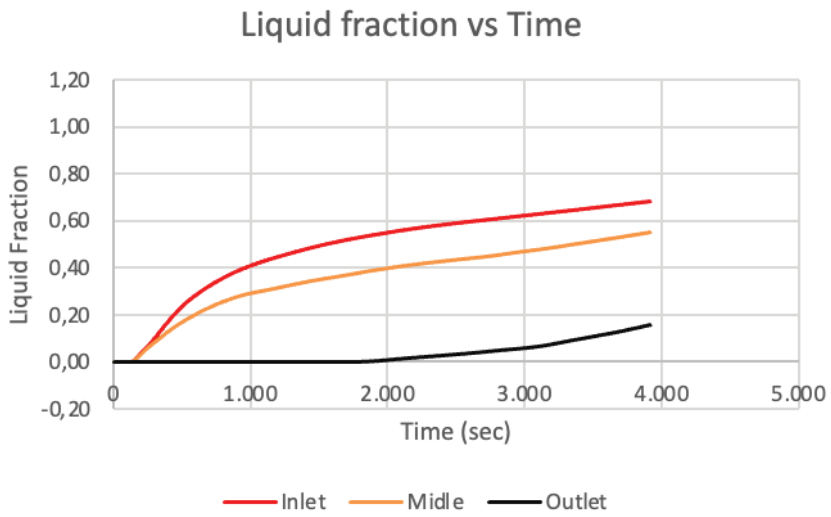

Figure 9. Variation of liquid fraction vs time for NEPCM storage material.

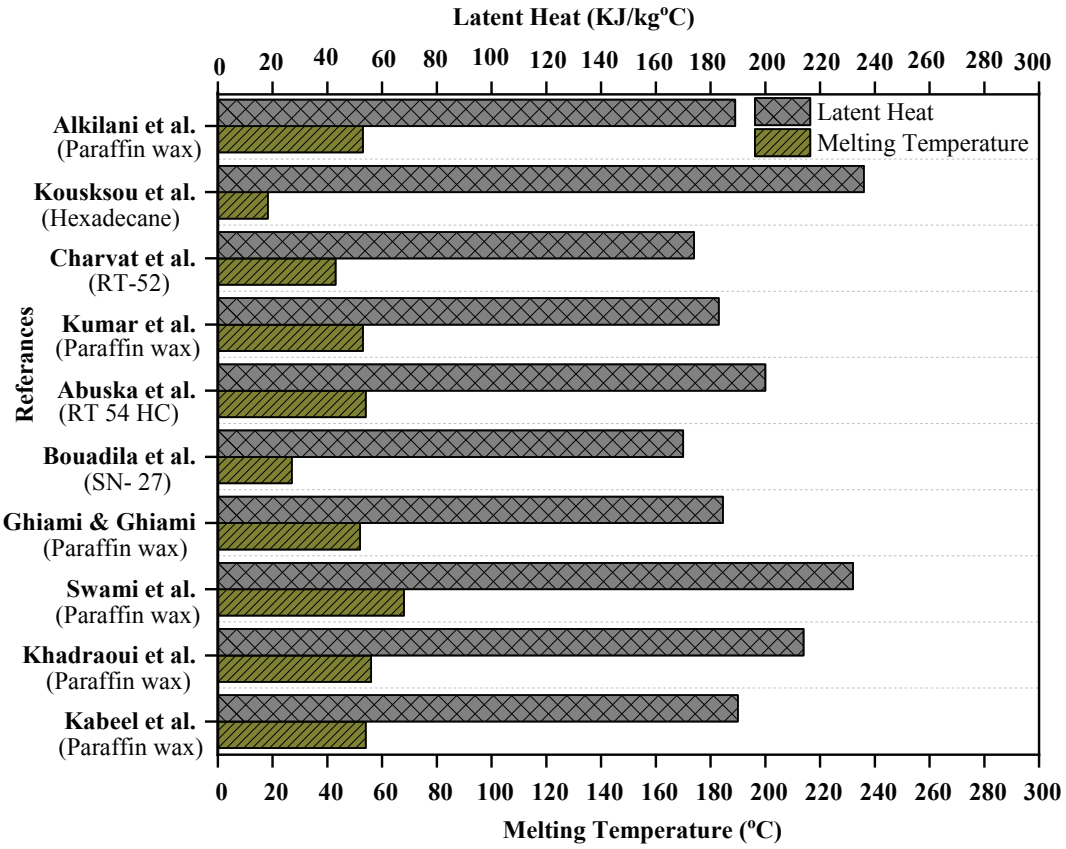

Figure 10. Various paraffin waxes concerning latent heat and melting temperature.

NEPCM system. Higher liquid fractions during melting can lead to faster energy absorption and shorter response times, making NEPCM suitable for applications that require rapid thermal energy storage or release.

Figure 10 exhibits the various types of paraffin wax utilized by the researchers, as well as analyses of latent heat and melting point. Because paraffin has limited heat conductivity, it must be used with a large heat transfer surface or heat transfer augmentation procedures [50–59].

CONCLUSION

An experimental investigation was carried out on a latent heat storage system, employing three different types of NEPCM with unique melting temperatures. To examine the impact of the heat transfer fluid flow rate on the charging and discharging processes, multiple experiments were conducted under different operational conditions.

Latent heat storage systems were studied in this experiment, and results are based on the usage of three different NEPCM samples with varying temperatures of melting. The effect of the solidification and melting process was analysed with different mass flow rate by taking into account a range of process parameters during the study. This section provides a brief overview of the study's most salient results.

- The observed increase in energy efficiency of the LHTESS with the rise in the heat transfer fluid flow rate to 3 lpm signifies a crucial optimization parameter. When the heat transfer fluid flow rate is increased to 3 LPM, the LHTESS energy efficiency increases from 54.72% to 74.35%.
- The intricate relationship between the charging and discharging rate of the PCM and the hot fluid flow rate is a key finding. A particle charge modulator's (PCM) charging and discharging rate is significantly affected by the hot fluid flow rate. The flow rate was increased from 1.0 to 5.0 LPM, resulting in a 10.0% reduction in melting time and a substantial 30.0% reduction in solidification time, respectively.
- The identified trade-off between mass flow rate and energy efficiency sheds light on the system's operational constraints and performance limitations. The energy efficiency decreased from 21.43% to 15.37% when the mass flow rate increased from 1.0 to 5.0 LPM.
- Results from this study suggest that compared to employing a single PCM, utilizing multiple PCMs can increase the energy storage capacity of an LHTES system. In conclusion, the storage capacity of the thermal energy storage system is improved by employing multilayer PCM.
- As the volume percentage of nano-particles increases in the PCM, heat transfer increases.
- Using nanoparticles increases the melting rate, which correlates directly to the volume fraction. ZrO_2 has better performance than the other nanoparticles because it has a greater thermal conductivity.
- Increased thermal conductivity from nanocomposites improves heat transfer throughout the PCM.
- Chemical energy storage materials are still in their initial stage. Therefore, more study is required for industrial applications.
- To supply practical solar thermal energy storage technologies, environmental-economic-exergy analysis needs to be given greater consideration.
- The use of PCM-integrated water tanks should be explored to keep temperatures lower during the day and higher at night depending on the environmental circumstances.
- Double-layer shell encapsulated PCM can be explored to widen the absorption spectra of solar radiation for enhanced energy absorption and storage capacity.
- Micro-nano-encapsulated materials can be used as building envelopes to reduce cooling and heating loads. This area requires consistent development of technologies and advanced engineering skills.

AUTHORSHIP CONTRIBUTIONS

Authors equally contributed to this work.

DATA AVAILABILITY STATEMENT

The authors confirm that the data that supports the findings of this study are available within the article. Raw data that support the finding of this study are available from the corresponding author, upon reasonable request.

CONFLICT OF INTEREST

The authors declared that they have no conflict of interests with any organization or persons.

ETHICS

There are no ethical issues with the publication of this manuscript.

REFERENCES

[1] Kumar B. Fossil energy reduction for heating and cooling of buildings using shallow geothermal integrated energy systems - a comprehensive review. J Therm Eng 2023;9:1386-1417. [CrossRef]

[2] Al-Yasiri Q, Szabó M. Paraffin as a phase change material to improve building performance: An overview of applications and thermal conductivity enhancement techniques. Renew Energy Environ Sustain 2021;6:38. [CrossRef]

[3] Hayat MA, Chen Y. A brief review on nano phase change material-based polymer encapsulation for thermal energy storage systems. In: Mporas I, Kourtessis P, Al-Habaibeh A, Asthana A, Vukovic V, Senior J, eds. Energy and Sustainable Futures. Cham: Springer, 2021. pp. 19-26.

[4] Punniakodi BMS, Senthil R. Recent developments in nano-enhanced phase change materials for solar thermal storage. Sol Energy Mater Sol Cells 2022;238:111629. [CrossRef]

[5] Singh SK, Verma SK, Kumar R. Thermal performance and behavior analysis of SiO2, Al2O3 and MgO based nano-enhanced phase-changing materials, latent heat thermal energy storage system. J Energy Storage 2022;48:103977. [CrossRef]

[6] Singh SK, Verma SK, Kumar R, Sharma A, Singh R, Tiwari N. Experimental analysis of latent heat thermal energy storage system using encapsulated multiple phase-change materials. Proc Inst Mech Eng Part E J Process Mech Eng 2022:09544089221110983. [CrossRef]
[7] Al-Absi ZA, Mohd Isa MH, Ismail M. Phase change materials (PCMs) and their optimum position in building walls. Sustainability 2020;12:1294. [CrossRef]
[8] Qin H, Wang Z, Heng W, Liu Z, Li P. Numerical study of melting and heat transfer of PCM in a rectangular cavity with bilateral flow boundary conditions. Case Stud Therm Eng 2021;27:101183. [CrossRef]
[9] Muhammed MD, Badr O. Analysis of a hybrid cascaded latent/sensible storage system for parabolic-trough solar thermal plants. J Therm Eng 2021;7:608-622. [CrossRef]
[10] Al-Kayiem HH, Lin SC, Lukmon A. Review on nanomaterials for thermal energy storage technologies. Nanosci Nanotechnol Asia 2021;3:60-71. [CrossRef]
[11] Alktranee M, Shehab MA, Németh Z, Bencs P, Hernadi K. Effect of zirconium oxide nanofluid on the behaviour of photovoltaic-thermal system: An experimental study. Energy Rep 2023;9:1265-1277. [CrossRef]
[12] Yuan H, Shi Y, Xu Z, Lu C, Ni Y, Lan X. Influence of nano-ZrO2 on the mechanical and thermal properties of high temperature cementitious thermal energy storage materials. Constr Build Mater 2013;48:6-10. [CrossRef]
[13] Huang Y, Yang S, Aadmi M, Wang Y, Karkri M, Zhang Z. Numerical analysis on phase change progress and thermal performance of different roofs integrated with phase change material (PCM) in Moroccan semi-arid and Mediterranean climates. Build Simul 2022;16:69-85. [CrossRef]
[14] Munir MU, Hussain A. Thermal stability analysis of a PCM-based energy storage system. Available at: https://www.mdpi.com/2673-4591/23/1/20/htm. Accessed Nov 12, 2022. [CrossRef]
[15] Waqas A, Ud Din Z. Phase change material (PCM) storage for free cooling of buildings-a review. Renew Sustain Energy Rev 2013;18:607-625. [CrossRef]
[16] Singh VP, Jain S, Karn A, Dwivedi G, Kumar A, Mishra S, Sharma NK, Bajaj M, Zawbaa HM, Kamel S. Heat transfer and friction factor correlations development for double pass solar air heater artificially roughened with perforated multi-V ribs. Case Stud Therm Eng 2022;39:102461. [CrossRef]
[17] Singh R, Sadeghi S, Shabani B. Thermal conductivity enhancement of phase change materials for low-temperature thermal energy storage applications. Energies 2019;12:75. [CrossRef]
[18] Purohit BK, Sistla VS. Studies on solution crystallization of Na2SO4·10H2O embedded in porous polyurethane foam for thermal energy storage application. Thermochim Acta 2018;668:9-18. [CrossRef]
[19] Herbinger F, Bhouri M, Groulx D. Investigation of heat transfer inside a PCM-air heat exchanger: A numerical parametric study. Heat Mass Transf 2018;54:2433-2442. [CrossRef]
[20] Sun X, Zhu Z, Fan S, Li J. Thermal performance of a lightweight building with phase change material under a humid subtropical climate. Energy Built Environ 2022;3:73-85. [CrossRef]
[21] Fateh A, Borelli D, Devia F, Weinläder H. Summer thermal performances of PCM-integrated insulation layers for light-weight building walls: Effect of orientation and melting point temperature. Therm Sci Eng Prog 2018;6:361-9. [CrossRef]
[22] Kishore RA, Bianchi MVA, Booten C, Vidal J, Jackson R. Parametric and sensitivity analysis of a PCM-integrated wall for optimal thermal load modulation in lightweight buildings. Appl Therm Eng 2021;187:116568. [CrossRef]
[23] Zwanzig SD, Lian Y, Brehob EG. Numerical simulation of phase change material composite wallboard in a multi-layered building envelope. Energy Convers Manag 2013;69:27-40. [CrossRef]
[24] Parrado C, Cáceres G, Bize F, Bubnovich V, Baeyens J, Degrève J, Zhang HL. Thermo-mechanical analysis of copper-encapsulated NaNO3-KNO3. Chem Eng Res Des 2015;93:224-231. [CrossRef]
[25] Wang H, Lu W, Wu Z, Zhang G. Parametric analysis of applying PCM wallboards for energy saving in high-rise lightweight buildings in Shanghai. Renew Energy 2020;145:52-64. [CrossRef]
[26] Rothan YA. Thermal analysis for solidification of PCM including nanoparticles within a container. Case Stud Therm Eng 2022;33:101920. [CrossRef]
[27] Arena S, Casti E, Gasia J, Cabeza LF, Cau G. Numerical simulation of a finned-tube LHTES system: Influence of the mushy zone constant on the phase change behaviour. Energy Procedia 2017;126:517-524. [CrossRef]
[28] Youssef W, Ge YT, Tassou SA. CFD modelling development and experimental validation of a phase change material (PCM) heat exchanger with spiral-wired tubes. Energy Convers Manag 2018;157:498-510. [CrossRef]
[29] Zhou G, Yang Y, Wang X, Cheng J. Thermal characteristics of shape-stabilized phase change material wallboard with periodical outside temperature waves. Appl Energy 2010;87:2666-2672. [CrossRef]
[30] Wołoszyn J, Szopa K, Czerwiński G. Enhanced heat transfer in a PCM shell-and-tube thermal energy storage system. Appl Therm Eng 2021;196:117332. [CrossRef]
[31] Arena S, Casti E, Gasia J, Cabeza LF, Cau G. Numerical analysis of a latent heat thermal energy storage system under partial load operating conditions. Renew Energy 2018;128:350-361. [CrossRef]

[32] Vérèz D, Borri E, Crespo A, Mselle BD, de Gracia Á, Zsembinszki G, Cabeza LF. Experimental study on two PCM macro-encapsulation designs in a thermal energy storage tank. Appl Sci 2021;11:6171. [CrossRef]
[33] Korody J, Dinesha P. Performance comparison of phase change materials for thermal energy storage. Mater Sci Forum 2017;909:231-236. [CrossRef]
[34] Williams JD, Peterson GP. A review of thermal property enhancements of low-temperature nano-enhanced phase change materials. Available at: https://www.mdpi.com/2079-4991/11/10/2578. Accessed Nov 12, 2022. [CrossRef]
[35] Qian Z, Shen H, Fang X, Fan L, Zhao N, Xu J. Phase change materials of paraffin in H-BN porous scaffolds with enhanced thermal conductivity and form stability. Energy Build 2018;158:1184-1188. [CrossRef]
[36] Wang J, Xie H, Xin Z. Thermal properties of paraffin based composites containing multi-walled carbon nanotubes. Available at: https://www.sciencedirect.com/science/article/abs/pii/S0040603109000616. Accessed Sep 05, 2021.
[37] Bose P, Amirtham VA. A review on thermal conductivity enhancement of paraffinwax as latent heat energy storage material. Renew Sustain Energy Rev 2016;65:81-100. [CrossRef]
[38] Helvaci HU, Khan ZA. Heat transfer and entropy generation analysis of HFE 7000-based nanorefrigerants. Int J Heat Mass Transf 2017;104:318-327. [CrossRef]
[39] Wang J, Xie H, Xin Z. Thermal properties of paraffin-based composites containing multi-walled carbon nanotubes. Thermochim Acta 2009;488:39-42. [CrossRef]
[40] Qian Z, Shen H, Fang X, Fan L, Zhao N, Xu J. Phase change materials of paraffin in H-BN porous scaffolds with enhanced thermal conductivity and form stability. Energy Build 2018;158:1184-8. [CrossRef]
[41] Bose P, Amirtham VA. A review on thermal conductivity enhancement of paraffin wax as latent heat energy storage material. Renew Sustain Energy Rev 2016;65:81-100. [CrossRef]
[42] Helvaci HU, Khan ZA. Heat transfer and entropy generation analysis of HFE 7000-based nanorefrigerants. Int J Heat Mass Transf 2017;104:318-327. [CrossRef]
[43] Benli H, Durmuş A. Performance analysis of a latent heat storage system with phase change material for new designed solar collectors in greenhouse heating. Sol Energy 2009;83:2109-2119. [CrossRef]
[44] Fuxin N, Long N, Yang Y, Shiming D. Cool storage performance of integrated heat pump system with triple-sleeve energy storage exchanger. Energy Procedia 2012;14:1896-1902. [CrossRef]
[45] Jurinak JJ, Abdel-Khalik SI. Properties optimization for phase-change energy storage in air-based solar heating systems. Sol Energy 1978;21:377-383. [CrossRef]
[46] Sarbu I, Sebarchievici C. A comprehensive review of thermal energy storage. Sustainability 2018;10:191. [CrossRef]
[47] Tambunan AH, Manalu LP, Abdullah K. Exergy analysis on simultaneous charging and discharging of solar thermal storage for drying application. Drying Technol 2010;28:1107-1112. [CrossRef]
[48] Venkitaraj KP, Suresh S, Praveen B. Experimental charging and discharging performance of alumina-enhanced pentaerythritol using a shell and tube TES system. Sustain Cities Soc 2019;51:101767. [CrossRef]
[49] Cho H, Smith A, Luck R, Mago PJ. Transient uncertainty analysis in solar thermal system modeling. J Uncertainty Anal Appl 2017;5:1. [CrossRef]
[50] Kabeel AE, Khalil A, Shalaby SM, Zayed ME. Improvement of thermal performance of the finned plate solar air heater by using latent heat thermal storage. Appl Therm Eng 2017;123:546-553. [CrossRef]
[51] Swami VM, Autee AT, TR A. Experimental analysis of solar fish dryer using phase change material. J Energy Storage 2018;20:310-315. [CrossRef]
[52] Abuşka M, Şevik S, Kayapunar A. A comparative investigation of the effect of honeycomb core on the latent heat storage with PCM in solar air heater. Appl Therm Eng 2019;148:684-693. [CrossRef]
[53] Bouadila S, Kooli S, Lazaar M, Skouri S, Farhat A. Performance of a new solar air heater with packed-bed latent storage energy for nocturnal use. Appl Energy 2013;110:267-275. [CrossRef]
[54] Ghiami A, Ghiami S. Comparative study based on energy and exergy analyses of a baffled solar air heater with latent storage collector. Appl Therm Eng 2018;133:797-808. [CrossRef]
[55] El Khadraoui A, Bouadila S, Kooli S, Farhat A, Guizani A. Thermal behavior of indirect solar dryer: Nocturnal usage of solar air collector with PCM. J Cleaner Prod 2017;148:37-48. [CrossRef]
[56] Charvát P, Klimeš L, Ostrý M. Numerical and experimental investigation of a PCM-based thermal storage unit for solar air systems. Energy Build 2014;68:488-497. [CrossRef]
[57] Kumar N, Gupta SK, Sharma VK. Application of phase change material for thermal energy storage: An overview of recent advances. Mater Today Proc 2021;44:368-375. [CrossRef]
[58] Kousksou T, Strub F, Castaing Lasvignottes J, Jamil A, Bédécarrats JP. Second law analysis of latent thermal storage for solar system. Sol Energy Mater Sol Cells 2007;91:1275-1281. [CrossRef]
[59] Alkilani MM, Sopian K, Mat S, Alghoul M. Output air temperature prediction in a solar air heater integrated with phase change material. Eur J Sci Res 2009;27:334-341.